Synthesis and Biological Activity of Photopolymerizable Derivatives of Glyphosate†

Aneta Bogdanova,‡ Victoria Piunova,‡ Daniel Berger,‡,|| Andrei V. Fedorov,*,§ and Douglas C. Neckers*,‡

Center for Photochemical Sciences and Wright Photoscience Laboratory, Bowling Green State University, Bowling Green, Ohio 43403

Received May 15, 2006; Revised Manuscript Received September 27, 2006

The synthesis of new acrylate and methacrylate derivatives of a glyphosate is reported. Two isomers resulting from a hindered rotation around the amide C−N bond are observed for both acrylic and methacrylic analogs, and barriers for internal rotation are obtained. Biological activity tests indicate that functionalized glyphosates possess herbicidal activity similar to that of the parent compound. Only the acrylated glyphosate derivatives undergo photopolymerization. The resulting photopolymer of acrylated glyphosate retains the biological activity. The methacrylated glyphosates are unreactive. Differential reactivity is explained by the different conformational preferences of the functionalized glyphosates. The experimental findings are supported by the results of density functional theory geometry optimizations.

Introduction

Photopolymerization holds two basic advantages over other routes of converting a liquid to a solid. The initiating stimulus (light) can be turned on or off so, for the most part, whether or not a polymerization occurs can be controlled. Light can also be imaged. Where light impinges on a to-be-polymerized monomer or oligomer mixture, polymerization occurs. Where it does not, there is no reaction. Nevertheless and somewhat surprisingly, only a limited number of photopolymerization processes have impacted the life sciences. Though photopolymerized gels for electrophoresis have been known since the 1950s and various monomer/oligomer formulations are used in dental applications, photopolymers that are used in other applications to encapsulate or coat have not been used to encapsulate biologically active compounds or coat surfaces with biological attractants/repellants. There are no known examples of which we are aware in which one has prepared an imaged surface with a bioattractant or repellant in the context of the *biophotoresist*—an effective biologically active compound imaged on a surface at the level of pixel resolution. In this paper we deal with this opportunity.

N-(Phosphonomethyl)glycine (glyphosate) **1** is a broad action, nonselective systematic herbicide that kills many annual or perennial grasses and broadleaf weeds as well as many species of trees and brush. The basis of the herbicidal activity of glyphosate is its quick penetration into a plant's leaves where it efficiently disrupts the synthesis of essential amino acids needed for protein generation. Glyphosate is generally used commercially in the form of its isopropylammonium salt, was marketed and originally patented by Monsanto, and is known by the trade name Roundup.[1,2]

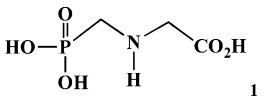

1

Despite the broad use of glyphosate in agriculture, little is known about its chemical reactivity, and only a small number of glyphosate derivatives have been reported.[3] Glyphosate is trifunctional, and each individual functionality is difficult to convert in the absence of reactions of the others, which partially explains its lack of study. As a part of a program targeting bioreactive photopolymers, we sought to prepare acrylic and methacrylic acid derivatives of glyphosate, convert them to polymers, and test their biological activities.

This paper reports the synthesis of a new class of photopolymerizable derivatives of glyphosate with herbicidal activity. The synthetic route to acrylic and methacrylic acid derivatives given in Scheme 1 appears trivial at first glance, however, is anything but in practice.

Experimental Section

Materials. *N*-(Phosphonomethyl)glycine was obtained from Aldrich and used as received. Acryloyl chloride (Aldrich) and methacryloyl chloride (Alfa Aesar) were distilled prior to use. Darocur 1173 and Irgacure 651 were obtained from Ciba Specialty Chemicals, Inc. The water-soluble diazo initiators VA-086, VA-085, and VA-057 were gifts from Wako Pure Chemical Industries, Ltd.

General Procedures. NMR spectra were recorded on either Varian Unity 400 MHz or Bruker Avance 300 MHz spectrometers. The NMR experiments at elevated temperatures were carried out on a Varian Unity 400 MHz spectrometer. All NMR spectra were recorded in D_2O, and chemical shifts are reported in ppm and referenced to 3-(trimethylsilyl)-propionic acid-d_4, sodium salt (TSP). Fourier transform infrared (FTIR) spectra were recorded on a ThermoNicolet IR200 spectrometer. High-resolution mass spectral analyses were performed by the Mass Spectrometry Laboratory, University of Illinois at Urbana−Champaign.

Polymerization Experiments. Polymerizations were carried out by irradiation of 17% solutions of glyphosate derivatives in D_2O in the presence of 1.5 wt % initiator using a RMR-600 Rayonet photochemical

† Contribution number 700 from the Center for Photochemical Sciences.

* Authors to whom correspondence should be addressed. E-mail: avfedor@bgnet.bgsu.edu; neckers@photo.bgsu.edu.

‡ Center for Photochemical Sciences, Bowling Green State University.

§ Wright Photoscience Laboratory, Bowling Green State University.

|| Permanent address: Science Department, Bluffton College, Bluffton, OH 45817.

10.1021/bm060477o CCC: $37.00
Published on Web 01/06/2007

Scheme 1

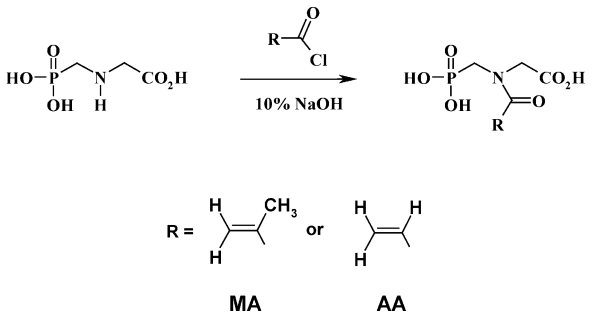

reactor equipped with seven lamps (λ_{ex} = 350 nm). The double bond conversion of monomer was followed by ^{1}H NMR using the TSP signal as the internal standard.

The molecular weight of the resulting photopolymer was determined using size exclusion chromatography (SEC). The Waters HPLC system (two 515 pumps and 996 diode array detector) was equipped with a Superdex 200 column from Amersham Biosciences with 1−100 kDa separation range. The polymer sample was dissolved in phosphate buffer with pH 7 (50 mM KH_2PO_4 and 100 mM KCl) and eluted through the column at 1 mL/min with detection at 210 nm. The molecular mass of the resulting polymer was determined using the calibration line obtained from analyzing solutions of dextranes having different molecular masses (Supporting Information).

Synthesis of *N*-Methacryloyl-*N*-(phosphonomethyl)glycine. The synthesis of *N*-methacryloyl-*N*-(phosphonomethyl)glycine (MA) was carried out according to the method reported by Gough[4] with several modifications. *N*-(Phosphonomethyl)glycine (0.169 g, 1 mmol) was dissolved in 2.4 mL of 10% sodium hydroxide solution. Then, to a vigorously stirred solution, methacryloyl chloride (0.146 mL, 1.5 mmol) was added under argon dropwise. After continuous stirring for 4 h at room temperature, the reaction mixture was acidified with hydrochloric acid to pH 0 or below and concentrated under vacuum to precipitate the NaCl, which was removed by filtration. The pH of the filtrate was then adjusted to 1−2 by adding sodium hydroxide solution. Further concentration of the reaction mixture yielded white precipitate, which was filtered and dried under vacuum to afford MA as a white solid (0.189 g, 40% (the yield is adjusted to the maximum possible residual NaCl content)). ^{1}H NMR (400 MHz, D_2O, δ/ppm): 1.90 (s, 3H, CH_3), 1.95 (s, 3H, CH_3), 3.82 (d, $^2J_{HP}$ = 12 Hz, 2H, CH_2−P), 3.87 (d, $^2J_{HP}$ = 12 Hz, 2H, CH_2−P), 4.32 (s, 2H, CH_2), 4.48 (s, 2H, CH_2), 5.12 (s, 1H, HC=C), 5.29 (s, 1H, HC=C), 5.32 (s, 1H HC=C), 5.41 (s, 1H, HC=C). ^{13}C NMR (75 MHz, D_2O, δ/ppm): 19.52 (CH_3), 19.63 (CH_3), 43.44 (d, $^1J_{PC}$ = 147 MHz, −CH_2−P), 47.98 (d, $^1J_{PC}$ = 147 MHz, −CH_2−P), 48.54 (−*C*H_2−C=O), 51.64(−*C*H_2−C=O), 117.63 (*C*H_2=C−), 118.30 (*C*H_2=C−), 138.82 (CH_2=*C*−),139.28 (CH_2=*C*−), 172.64 (CH_2−*C*=O), 173.30, (CH_2−*C*=O) 175.90, (N−C=O) 176.45 (N−C=O). IR (neat, cm^{-1}): 1720, 1678, 1590, 1462, 1406. HRMS (ES^+) Calcd. for $C_7H_{13}NO_6P$ $[M + H]^+$: 238.0481. Found: 238.0487.

Synthesis of *N*-Acryloyl-*N*-(phosphonomethyl)glycine. *N*-Acryloyl-*N*-(phosphonomethyl)glycine (AA) was synthesized using a similar procedure to that described for MA. Acryloyl chloride was used in 2-fold excess relative to the concentration of glyphosate. The reaction was completed in 1 h to give AA as a white solid in 50% yield. (The yield is adjusted to the maximum possible residual NaCl content.) ^{1}H NMR (300 MHz, D_2O, δ/ppm): 3.95 (d, $^2J_{HP}$ = 12 Hz, 2H, CH_2−P), 3.98 (d, $^2J_{HP}$ = 12 Hz, 2H, CH_2−P), 4.29 (s, 2H, CH_2), 4.50 (s, 2H, CH_2), 5.87 (dd, AMX system, J_{AX} = 10.8 Hz, J_{AM} = 1.2 Hz, 1H, H_2C=CH), 5.93 (dd, AMX system, J_{AX} = 10.8 Hz, J_{AM} = 1.2 Hz, 1H, H_2C=CH), 6.25 (dd, AMX system, J_{MX} = 16.8 Hz, J_{MA} = 1.2 Hz, 1H, H_2C=CH), 6.29 (dd, AMX system, J_{MX} = 16.8 Hz, J_{MA} = 1.2 Hz, 1H, H_2C=CH), 6.61 (dd, AMX system, J_{XM} = 16.8 Hz, J_{XA} = 10.8 Hz, 1H, H_2C=C*H*), 6.82 (dd, AMX system, J_{XM} = 16.8 Hz, J_{XA} = 10.8 Hz, 1H, H_2C=C*H*). ^{13}C NMR (75 MHz, D_2O, δ/ppm): 44.24 (d, $^1J_{PC}$ = 150 MHz, −CH_2−P), 46.73 (d, $^1J_{PC}$ = 150 MHz, −CH_2−P), 50.04

Scheme 2

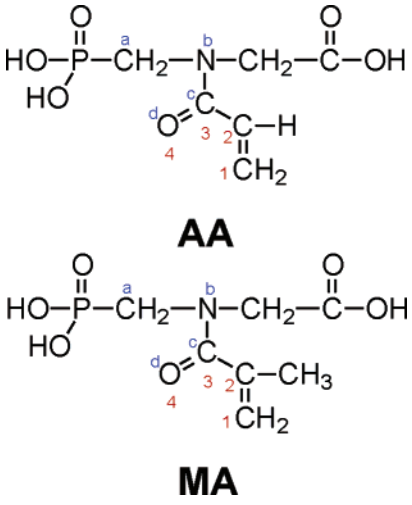

(−*C*H_2−C=O), 50.74 (−*C*H_2−C=O), 126.86 (*C*H_2=C−), 126.96 (*C*H_2=C−), 130.27 (CH_2=*C*−), 130.65 (CH_2=*C*−), 169.94 (CH_2−*C*=O), 169.96 (CH_2−*C*=O), 172.66 (N−C=O), 172.75 (N−C=O). IR (neat, cm^{-1}): 1722, 1637, 1571, 1472, 1401. HRMS (ES^+) Calcd. for $C_6H_{11}NO_6P$ $[M + H]^+$: 224.0324. Found: 224.0330. Calcd. for $C_6H_{10}NO_6PNa$ $[M + Na]^+$: 246.0140. Found: 246.0142.

Determination of Residual Sodium Chloride Content. Residual solid content was estimated by heating a sample at red heat in a crucible for 30 min. Crucibles were weighed empty as well as with the sample both before and after heating. The amount of residual solids was determined for various batches of acrylated product and compared to those of the parent glyphosate. Typical values for the product were 35−45% by weight (versus 5−10% for technical-grade glyphosate). The major solid contaminant was sodium chloride, and the product gives a positive silver nitrate test when dissolved in distilled water. The maximum content of NaCl in the product was estimated at 40%.

Computational Methods. The compounds analyzed were AA and MA. Calculations were performed using Spartan 04 except for B3LYP/6-31++G(d,p)//B3LYP/6-31++G(d,p) calculations which were performed using Gaussian 03 (Supporting Information). PM3 semiempirical calculations and density functional methods with diffuse basis sets were used to keep the structures from losing their hydrogen-bonded character during optimization.

Structures were selected to maximize hydrogen-bonding stabilization. Some structures were chosen in which the phosphoryl group was a hydrogen-bond donor to the acryloyl carbonyl, while the carboxyl group was a hydrogen-bond donor to the negative phosphoryl oxygen. Other structures were chosen with the carboxyl group as a hydrogen-bond donor to the acryloyl carbonyl, while the phosphoryl group was a hydrogen-bond donor to the carboxyl group (Scheme 2).

Rotational studies were performed in which one of two chosen dihedral angles was constrained to a series of values and the rest of the molecule was allowed to relax. Several series of structures were generated by constraining a certain dihedral angle—either the acryloyl C=C−C=O dihedral (1−2−3−4) or the amide C(P)−N−C=O dihedral (a−b−c−d)—and allowing the rest of the structure to relax by sequential molecular mechanics, PM3, and B3LYP/6-31G calculations. Geometries at and near the local minima identified by the rotational studies were fully optimized (no dihedral angle constraints) at the B3LYP/6-31+G*level.

Eight candidate local minima were found for MA, with vinyl dihedral angles of ±120−130° and ±40−60°. Amide dihedral angles were all within 15° of planarity. Nine candidate local minima were found for AA, with vinyl dihedral angles from −6° to +8°, from +127° to +132°, and from −126° to −132°. Candidate local minima were fully optimized at the B3LYP/6-31++G(d,p) level. The absence of imaginary frequencies from vibrational analysis confirmed that all structures found were indeed local minima.

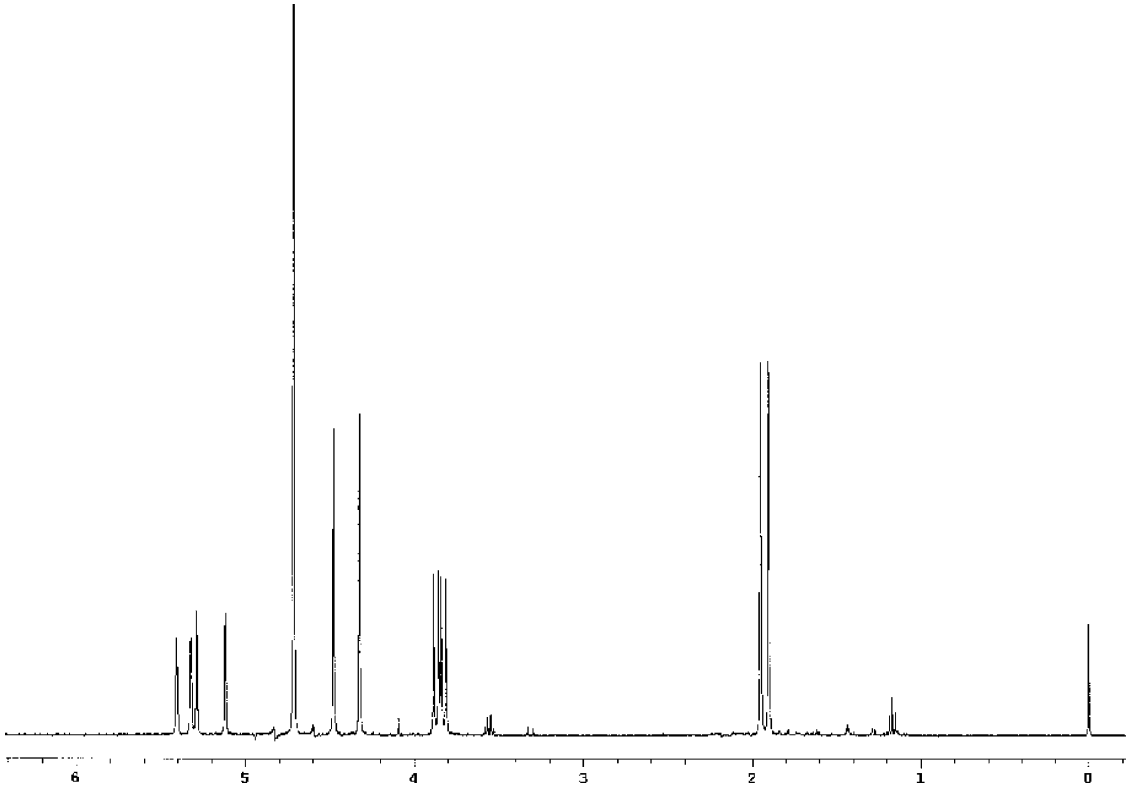

Figure 1. ^{1}H NMR spectrum of *N*-methacryloyl-*N*-(phosphonomethyl)glycine (MA).

Biological Activity Tests. *Materials and Methods.* The following materials were tested for biological activity: glyphosate (Monsanto Chemical Co.), acrylated glyphosate (AA), and poly(acrylated glyphosate). The biological activity of methacrylated glyphosate (MA) was not examined, but we expect results similar to the behavior of AA. Glyphosate and acrylated glyphosate were dissolved in doubly deionized water (200 mM (the concentration is adjusted for the maximum possible content of the residual NaCl in the AA)), and these stock solutions were used to prepare all relevant biological media. Polymerization of acrylated glyphosate was also conducted in aqueous media (350 nm irradiation with 1.5 wt % VA-085 initiator), with the same initial concentration of the monomer as for the unconverted AA experiments.

Strains of green algae, cyanobacteria, and *Escherichia coli* were used as test organisms. The green algae CD 1 Red and cyanobacteria *Synechocystos* 6803 were obtained from the collection of Professor George Bullerjahn. A salt water strain of cyanobacteria *Synechococcus* 7002 was obtained from the collection of Professor Michael McKay. *E. coli* DH5α was obtained from Invitrogen, Inc.

Media Preparation and Cell Growth Measurements. Green algae and cyanobacteria were propagated photoautotrophically in 250 mL Erlenmeyer flasks containing 100 mL of liquid BG-11 culture medium (Supporting Information). The cultures were kept on a rotating shaker (100 rpm) at 25 °C for 4 days and continuously illuminated with cool-white fluorescent light with a constant light intensity of 5000 lux. The grown culture medium was sterilized in an autoclave at 121 °C and 1.05 kg cm^{-2} of pressure for 20 min. For the cell experiments, 20 mL aliquots of the BG-11 medium containing the green algal ($[\text{cells}]_{\text{initial}} = 5.9 \times 10^7$ mL^{-1}) or cyanobacteria cells ($[\text{cells}]_{\text{initial}} = 1.7 \times 10^9$ mL^{-1}) were placed in sterile 50 mL Erlenmeyer flasks. CD 1 Red, *Synechocystos* 6803, and *Synechococcus* 7002 were then treated with an aliquot of a stock herbicide solution to bring the final herbicide concentration to 1 mM and incubated for 7 days on a rotator shaker (100 rpm) at 25 °C and a continuous light intensity of 5000 lux. Cell counts were correlated with the absorbance and measured as a function of time using a Spectronic 20 Genesis spectrophotometer. As previously reported by Ma et al.,[5] the optimal wavelength for monitoring culture growth is 680 nm. Experiments for each herbicide were repeated three times. Control and treated cultures were grown under the same conditions of temperature, photoperiod, and agitation. In each experiment, the inhibition of cell growth in treated cultures was monitored spectrophotometrically and compared to the growth in control samples.

E. coli was propagated heterotrophically in a 2 mL Eppendorf test tube containing 1.5 mL of liquid M9 minimum medium (Supporting Information) and kept on a rotating shaker (100 rpm) at 37 °C for 12 h. The growth culture medium was sterilized at 121 °C and 1.05 kg cm^{-2} for 20 min. For the cell experiments, 100 mL aliquots of the M9 medium containing the *E. coli* cells ($[\text{cells}]_{\text{initial}} = 6 \times 10^5$ mL^{-1}) were distributed into sterile 250 mL Erlenmeyer flasks and treated with a stock herbicide solution to obtain a final concentration of 30 mM, followed by an incubation for 24 h on a rotating shaker (100 rpm) at 37 °C. Cell counts were correlated with the absorbance at 600 nm over time using a Spectronic 20 Genesis spectrophotometer. Control and treated cultures were grown under the same conditions of temperature and shaking. In each experiment, the inhibition of growth in treated cultures was monitored spectrophotometrically and compared to the growth in the control samples.

Agar Experiments. BG-11 medium containing 1.5 wt % agar was prepared and sterilized at 121 °C and 1.05 kg cm^{-2} for 20 min. Each herbicide tested was prepared as a 30 mM solution and added to the autoclaved agar medium to yield a 1 mM final concentration of the herbicide. A 20 mL aliquot of the liquid agar was transferred into a standard Petri dish (100 × 15 mm) and allowed to harden at room temperature. Cell suspensions of green algae CD 1 Red, cyanobacteria *Synechocystos* 6803, and *Synechococcus* 7002 were inoculated using a sterile inoculation loop. Dishes were stored at 25 °C under illumination with the cool-white fluorescent light having a constant light intensity of 5000 lux. The experiment for each herbicide was repeated five times. Control and treated cultures grew under the same conditions of temperature and photoperiod. In each experiment, the inhibition of growth in treated cultures was monitored relative to the growth in control samples using qualitative visual observation.

Additional experiments for testing the toxicity of the homopolymer of AA were implemented. Approximately 10 mL of aqueous polymer solution was placed on a sterile Petri dish and left at room temperature until all water was evaporated (3 days) to form a thin polymer film. Approximately 20 mL of the liquid agar was transferred into the Petri

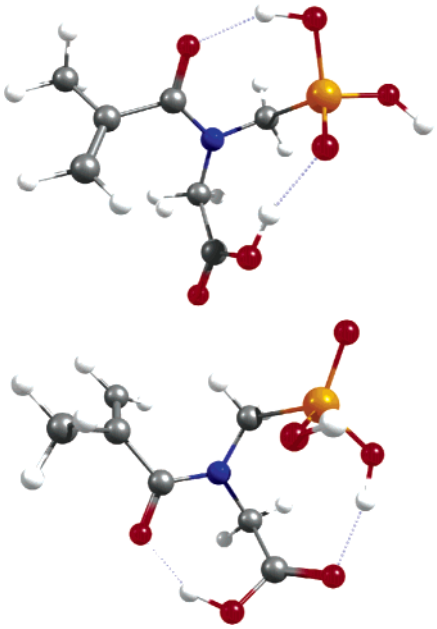

Figure 2. Two different isomers of MA.

dish and allowed to harden at room temperature. Cell suspensions of green algae CD 1 Red, cyanobacteria *Synechocystos* 6803, and *Synechococcus* 7002 were inoculated using a sterile inoculation loop. An analogous system containing no polymer film was used as a control for the experiment. Inhibition of growth in treated cultures was monitored relative to the growth in control samples using qualitative visual observations.

E. coli Agar Experiments. A M9 minimum medium containing 1.5 wt % agar was prepared and sterilized at 121 °C, 1.05 kg cm^{-2} for 20 min. An aliquot of each tested herbicide solution was added to portions of the autoclaved agar to give a 1 mM final concentration of the herbicide. Approximately 20 mL of the liquid agar was poured into a standard Petri dish and allowed to harden at room temperature. *E. coli* cell suspensions were inoculated using a sterile inoculation loop and stored at 37 °C for 24 h. Control and treated cultures were grown under the same conditions. In each experiment, the inhibition of growth in treated cultures was monitored relative to growth in control samples by manually counting the number of colonies.

Kirby−Bauer Experiments. The herbicidal activity of novel acrylated glyphosate and poly(acrylated glyphosate) as well as acrylamide and glyphosate (as controls) was also compared using the Kirby−Bauer disc diffusion method.[6] Filter paper circles ($d = 5$ mm) soaked with acrylated glyphosate, poly(acrylated glyphosate), glyphosate, and acrylamide solutions of given concentrations were placed on the Petri plates, loaded with a layer of BG-11 containing agar medium (1.5 wt %, 10 mL) and a layer of BG-11 containing low melting point agarose medium (0.8 wt %, 5 mL) previously seeded with green algae CD 1 Red (5.9×10^6 cell/mL, 2 mL) or cyanobacteria *Synechococcus* 7002 (1.7×10^8 cell/mL, 2 mL). After phototrophical propagation during the 5 days under cool fluorescent light (intensity 5000 lux), the average radii of the inhibition zones were measured. Water-soaked filter paper circles were used as controls. Experiments for each herbicide concentration were repeated three times.

Results and Discussion

Synthetic Considerations. Two major challenges that arise in the synthesis of glyphosate derivatives are its poor solubility in organic solvents and the presence of both acidic and basic functional groups in the same molecule. Glyphosate exists as a zwitterion.[7] The acid dissociation constants for glyphosate are pKa_1 0.8 (first phosphonic), pKa_2 2.3 (carboxylic), pKa_3 6.0 (second phosphonic), and pKa_4 11 (amine). Further, the carboxyl and phosphonyl groups are electrophilic, while the amino group is nucleophilic, while the double-bonded and deprotonated oxygens of the phosphonyl group are stabilized by delocalization, resulting in the phosphonyl group being less susceptible to a nucleophilic attack than the carboxyl group.

Attempts to utilize standard esterification routes were unsuccessful. *N*-(Phosphonomethyl)glycine was converted to the corresponding acyl chloride by reaction with thionyl chloride.[8] When followed by treatment with the hydroxyethylmethacrylate, a complex mixture, the NMR spectrum of which showed no olefinic signals, resulted. So the reaction products were not separated. Reaction of glyphosate with methacryloyl chloride also failed to yield the corresponding anhydride.

The successful procedure involved activating the glycine carboxylic acid functionality with chlorotrimethylsilane, thus forming the corresponding silyl ester. This glycine derivative then reacts with alcohols to generate the desired glyphosate esters that were isolated by treating the reaction mixture with propylene oxide.[9] Using this procedure we obtained the allyl ester of glyphosate in quantitative yield. Neverthless, all other efforts to prepare the more readily photopolymerizable anhydrides or esters, such as those of methacrylic or acrylic acid, were unsuccessful.

Preparation of the methacrylate amide of glyphosate was achieved as follows: *N*-(Phosphonomethyl)glycine was dissolved in an excess of 10% NaOH solution and subsequently treated with the corresponding acyl chloride to form the amide derivative. The challenge was the separation of the water-soluble glyphosate derivatives from the side product, NaCl. Because the reaction generated a substantial amount of NaCl (the reaction was carried out in a 6-fold excess of NaOH) and this had to be removed, we found that it could be managed using the differential solubilities of methacrylated or acrylated glyphosate derivatives and that of NaCl in water at different pH values. After the reaction was completed, the pH of the mixture was adjusted to below zero by adding concentrated hydrochloric acid. At pH 0, the solubility of NaCl is substantially lower than that of the target product, and the precipitated alkali metal salt was removed by filtration. The pH of the aqueous solution was then adjusted to 1−2 by adding NaOH solution. Concentration of the reaction mixture under vacuum led to the precipitation of the desired amide, which was substantially more pure. Similar observations have been made for the solubility of glyphosate, and a method for its isolation from aqueous alkali metal solutions has been previously proposed.[10] Despite our extensive efforts to reduce the NaCl content in the final product, the residual NaCl amount remains at approximately the 30−40% level.

NMR Spectroscopy. The NMR spectrum of the methacrylic acid derivative of glyphosate is shown in Figure 1. The ^{1}H NMR spectrum of *N*-methacryloyl-*N*-(phosphonomethyl)glycine (MA) in D_2O shows two identical sets of signals in a 1:1 ratio for all protons: two signals for the methyl group, two doublets for a methylene group attached to phosphorus, two singlets for a methylene group attached to the carboxylic group, and signals for two different double bonds. A similar situation is observed in the ^{13}C NMR spectra, where all signals are doubled. These complex spectra can be rationalized by the presence of two equally stable isomers of MA.

Amides are known to exist in two conformations owing to hindered rotation around the C−N bond, which possesses partial double bond character.[11,12] The existence of two isomers of MA in D_2O can also be explained by hindered rotation around the

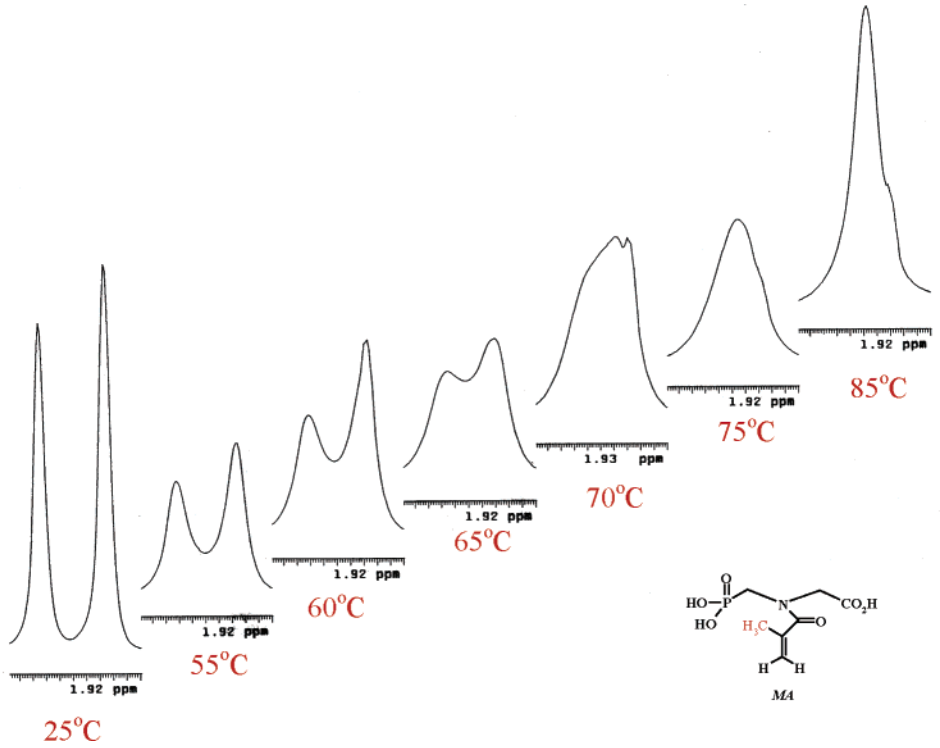

Figure 3. Temperature-dependent ^{1}H NMR spectra of MA.

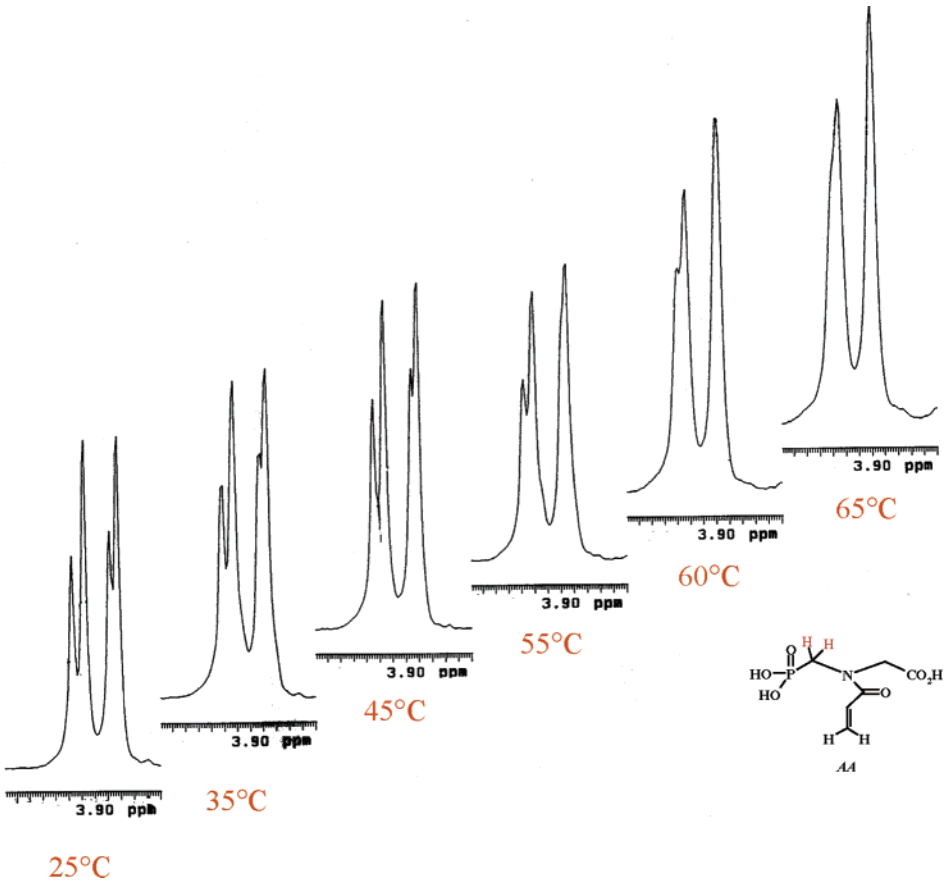

Figure 4. Temperature-dependent ^{1}H NMR spectra of AA.

C—N bond. Additional stabilization of MA isomers compared to dimethylformamide arises from the possibility of formation of two strong intramolecular hydrogen bonds (HBs). One HB is formed between the methacryloyl oxygen and either carboxylic or phosphonic hydrogen atoms while the second HB interaction occurs between the carboxylic C═O and the second OH group of the phosphonyl moiety (Figure 2). As revealed from the NMR spectra, both conformers are equally populated and, therefore, have similar stabilities.

It is interesting to note that the chemical shifts of the methacryloyl double bond signals appear at unusually high field (5.0−5.3 ppm). Typically, signals for this type of protons appear

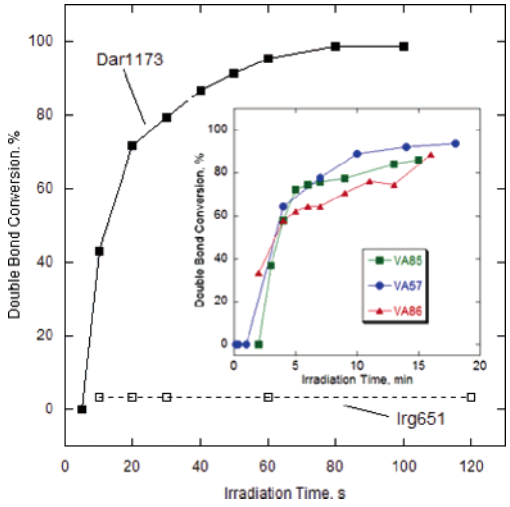

Figure 5. Polymerization of AA in the presence of different photoinitiators.

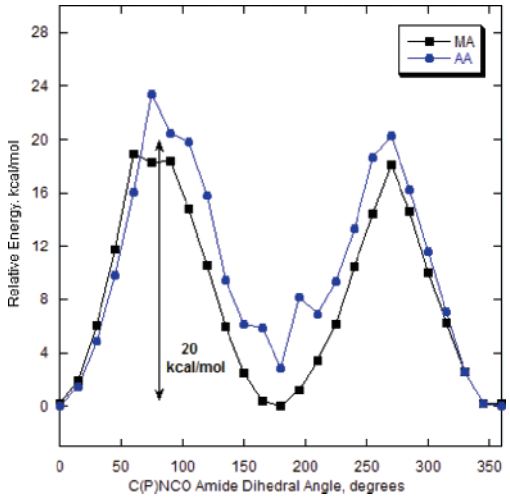

Figure 6. Results of C(P)−N−C═C amide bond rotational analysis for both AA and MA.

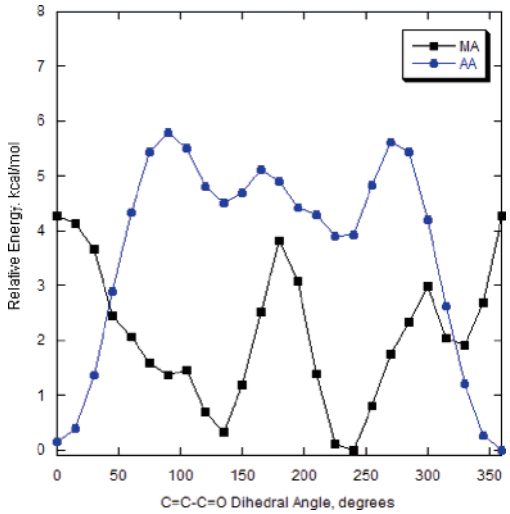

Figure 7. Results of C═C−C═O acryloyl bond rotational analysis for both AA and MA.

at about 5.5−6.0 ppm downfield of tetramethylsilane. This can be explained by the conformational preferences of MA that are governed by steric factors (vide infra).

Similarly to its methacrylated analog, *N*-acryloyl-*N*-(phosphonomethyl)glycine (AA) also exists as a mixture of two slowly exchanging conformers at room temperature. Both ^{1}H and ^{13}C NMR spectra of the acryloyl derivative contain two sets of signals for all protons or carbons, respectively (Supporting Information). Apparently, the relative stability of two AA conformers is not the same as that for MA, and the ratio between them is approximately 1:2. The signals from the AA double bond hydrogen in the ^{1}H NMR spectrum appear at substantially lower field compared to those of MA. In general, the electron-donating effect of a methyl group is expected to cause an upfield shift. For instance, the signals from the double bond terminal protons of methyl acrylate appear at 6.40 and 5.82 ppm,[13] while the parent signals for methyl methacrylate are at 6.09 and 5.55 ppm. This represents a 0.3 ppm difference in chemical shifts. For methacrylic and acrylic acids this difference is approximately 0.26 ppm. However, for methacrylic (MA) and acrylic (AA) acid derivatives of glyphosate this difference is nearly 1.5 ppm. This large difference is unlikely to be entirely due to the electron-donating abilities of the methyl group and can also be attributed to steric hindrance leading to conformational differences (vide infra).

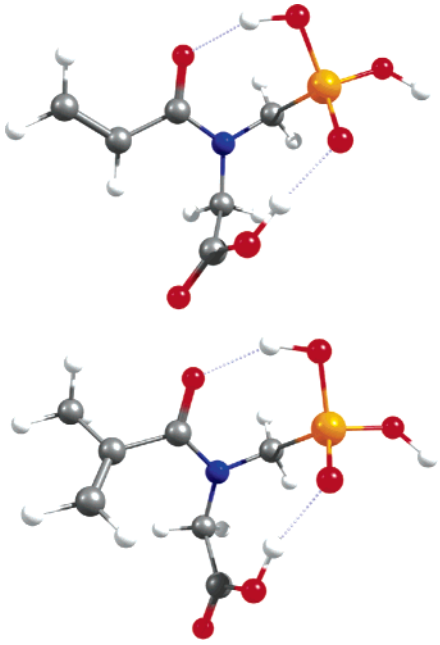

Figure 8. B3LYP/6-31++G(d,p) optimized structures of the lowest-energy isomers of AA (top) and MA (bottom).

Conformational Studies at Elevated Temperature. To further elucidate the conformational equilibria of MA and AA, the ^{1}H NMR signals of interest were observed at elevated temperatures. At room temperature, the ^{1}H NMR spectrum of MA shows two signals from the methyl groups at 1.90 and 1.95 ppm. Increasing the temperature causes a broadening of those signals, which completely merge at 75 °C (Figure 3). We observed broadening for all other signals in the NMR spectra although coalescence occurred only for methyl and methylene (CH_2−P) signals at temperatures up to 85 °C. The coalescence temperature for the methyl signals allows one to evaluate the barrier for conformer interconversion. The rate constant for a C—N bond rotation at the temperature of coalescence can be calculated according to the following expression[14]

$$k = \frac{2\pi(\nu_1 - \nu_2)}{\sqrt{2}}$$

where ν_1 and ν_2 are the chemical shifts in hertz at the slow exchange limit.

Table 1. Results of the Biological Activity Screening

organism	description	optical Density at 680 nm after 7 days of media growth		
		control	glyphosate	acrylic glyphosate (AA)
CD1 Red	green algae[a]	0.55	0.02	0.02
Synechocystos 6803	cyanobacteria (fresh water strain)[b]	1.4	0.58	0.54
Synechococcus 7002	cyanobacteria (salt water strain)[b]	0.72 (0.75 NaCl)	0.04	0.07
E. coli	bacteria[b]	1.30[c]	1.20[c]	1.24[c]

[a] Eukaryotic organism. [b] Prokaryotic organism. [c] Owing to a faster growth of *E. coli*, measurements were taken after 24 h of growth.

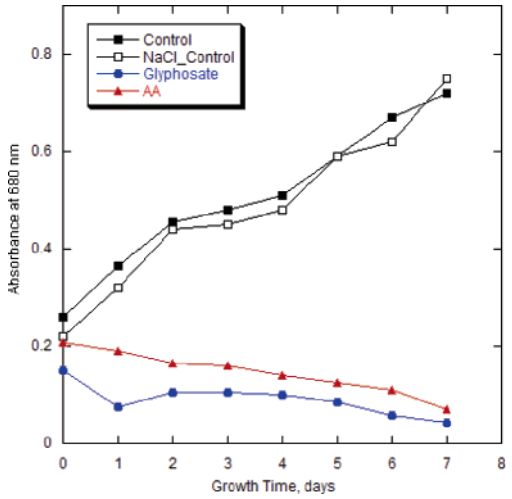

Figure 9. *Synechococcus* 7002 growth inhibition by the glyphosate and its acrylated derivative.

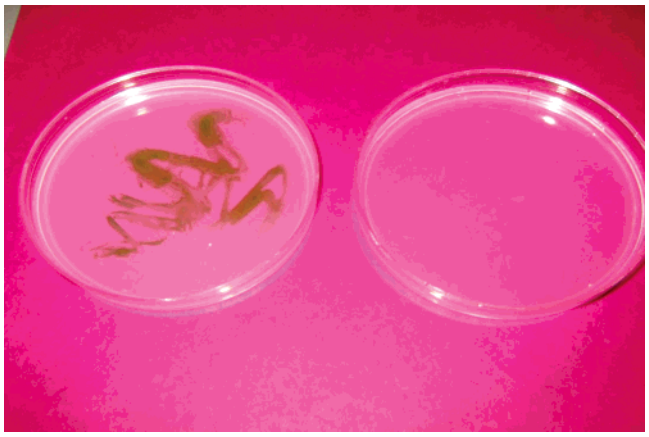

Figure 10. Results of the Kirby−Bauer test for the agar medium placed over the layer of AA homopolymer (right dish) and control (left dish).

Fitting the rate constant k in the Eyring equation gives the free energy of activation ($\Delta G^{\ddagger}$). Thus, for MA**,** we found the activation energy for conformational isomerism at 348 K to be 17.3 kcal/mol.

Evaluation of the barrier to internal rotation for AA was more difficult because we had to follow the temperature-dependent changes in more complex signals. The room temperature ^{1}H NMR spectrum of AA shows two doublets centered at 3.95 and 3.98 ppm assigned to the protons of the methylene group attached to phosphorus atom. The signals corresponding to each of the conformers can be easily distinguished from the $^2J_{HP}$ = 12 Hz coupling constant and the difference in their intensity. Figure 4 follows the changes in the methylene signals obtained from the temperature-dependent ^{1}H NMR spectra of AA. At elevated temperatures, the signals of the two doublets broaden and come closer to one another, and at 65 °C, they overlap to form one doublet ($^2J_{HP}$ = 12 Hz). The coalescence temperature allowed us to estimate the free energy of activation for the C−N bond rotation of AA ($\Delta G^{\ddagger}_{338\ K}$ = 17.9 kcal/mol). A similar value for the activation energy was found for MA conformational interconversion when we followed the methylene (CH_2−P) signals ($\Delta G^{\ddagger}_{358\ K}$ = 17.8 kcal/mol).

Photopolymerization Experiments. ^{1}H NMR spectroscopy was used to follow the photopolymerization of methacrylic and acrylic acid derivatives of glyphosate, MA, and AA. These compounds are soluble in water but are poorly soluble in most organic solvents. The polymerization experiments were carried out in deuterium oxide, using radical polymerization initiators. We introduced the marginally water-soluble initiators as an aliquot of a concentrated acetonitrile solution. The samples were then irradiated at 350 nm.

Surprisingly, MA did not polymerize under these conditions although we tried several Norrish type 1 and diazo initiators and long irradiation times. However, the acrylic analog AA polymerized efficiently. Figure 5 shows the conversion of the AA double bond using 1.5 wt % Darocur 1173 as the initiator. Over 95% conversion of the double bond was achieved in less than 80 s. The polymerization profile shows a typical autoacceleration effect, leading to an increase of the initial polymerization rate, followed by an autodeceleration effect.

The photopolymerization behavior of AA using Irgacure 651 (Figure 5), which has a 6 times higher molar extinction coefficient at 350 nm than Darocur 1173, showed an insignificant AA double bond conversion even after 7 min of irradiation. This is likely because of poor solubility of Irgacure 651 in water.

In an attempt to overcome these solubility issues, we also investigated photopolymerization rates with several water-soluble diazo initiators. The inset of Figure 5 shows that the polymerization profile of AA obtained using VA-057, VA-85, and VA-86 diazo initiators is slow but viable and the polymerization behavior of AA is similar in all three experiments. Double bond conversion of 80−90% is achieved after 15 min of irradiation. The polymerization time is considerably longer than that in the case of Darocur 1173. Although diazo initiators are more soluble in water, their absorption cross sections at 350 nm are half that of Darocur 1173, and they are also less efficient photoinitiators because the carbon radicals produced are not as reactive.

Owing to the high polarity of the AA monomer, SEC was used to determine the molecular weight of the resulting photopolymer. The SEC experiments yielded a molecular weight of 55 ± 10 kDa (Supporting Information).

The different photopolymerization behaviors of methacrylic (MA) and acrylic (AA) acid derivatives can be explained by the different conformational preferences of the two compounds. Generally, methacrylic acid derivatives, although they polymerize more slowly than their acrylic acid counterparts, still often undergo efficient polymerization with a high degree of double bond conversion. As discussed above, the signals from the double bond protons in the ^{1}H NMR spectrum of MA appear at unusually high field. Similarly, the double bond signals for *N*,*N*-dimethylmethacrylamide appear at 5.3 and 5.03 ppm.[13] We

Table 2. Average Radii of the Inhibition Zones Measured Around the Filter Paper Circles Treated with the Designated Compound

culture	herbicide concentration (mM)	inhibition by glyphosate (mm)	inhibition by acrylated glyphosate (mm)	inhibition by acrylamide (mm)	inhibition by polymer (mm)
Synechococcus 7002	0.3	no	no	no	9 (0.025 g/mL)
	3	6	no	no	13.5(0.25 g/mL)
	30	8	6.5	no	
	300	complete inhibition with bleaching	15	complete inhibition with bleaching	
CD1 Red	0.3	no	no	no	13 (0.025 g/mL)
	3	no	no	no	22 (0.25 g/mL)
	30	7.5	no	no	
	300	complete inhibition with bleaching	10	7.5	

submit that the steric bulk of the methyl group forces the MA molecule to adopt a conformation wherein the methacrylic C═O and C═C moieties are not coplanar. This prevents conjugation of the carbonyl group with the double bond, leading to deactivation of the double bond and its inability to undergo efficient polymerization under free radical polymerization conditions. Other N,N-disubstituted methacrylamides have also failed to polymerize under similar conditions.[15]

Computational Results. The conformational preferences in both AA and MA were further probed by the calculations. Only one series was evaluated for rotation of the amide C—N bond for both AA and MA, since whether the methacryloyl or acryloyl carbonyl can accept hydrogen bonds from the phosphoryl or the carboxyl group will depend on the value of the dihedral angle (Figure 6). Two global minima were identified for dihedral angles of ca. 0° (P—OH···O═C HB) and ca. 180° (COOH···O═C HB), with the dihedral angle defined as C(P)—N—C═O (a—b—c—d) (Scheme 2). High-level geometry optimization for two isomers favors the 0° isomer by 2.2 and 3.7 kcal/mol for MA and AA, respectively. The observed larger difference in stability of AA conformers is consistent with the experimentally observed difference in the NMR signal ratios for MA (1:1) and AA (2:1).

Our calculations show that the values of the barrier for rotation around the C—N bond of MA and AA are quite similar. This suggests that rotation around the C—N bond in MA is not hindered by the methyl group. For both MA and AA, the calculated value for the rotational barrier is approximately 20 kcal/mol (Figure 6). This value is in good agreement with the experimental barrier of 17—18 kcal/mol determined from the elevated temperature NMR experiments.

Two structural series were generated by rotating the vinyl group of the methacryloyl moiety, with hydrogen-bond donation to the methacryloyl carbonyl from either the phosphoryl group or the carboxyl group. Possible local minima were identified at ca. 135° and ca. 240° for both series, with the dihedral angle defined as C═C—C═O (1—2—3—4) (Scheme 2). All identified local minima had methacryloyl dihedral angles (1—2—3—4) of roughly ±120° (Figure 7). The two lowest-energy minima found had calculated energies within 200 cal of each other and methacryloyl dihedral angles of −123° and +121°.

Structural series were also generated by rotating the vinyl group of the acryloyl moiety of AA, with hydrogen-bond donation to the acryloyl carbonyl from either the phosphoryl group or the carboxyl group. Possible local minima were identified at ca. 0°, ca. 135°, and ca. 240° for both series, with the dihedral angle defined as C═C—C═O (1—2—3—4) (Scheme 2). Another possible local minimum was identified at 60° for the series in which the carboxyl group served as the hydrogen-bond donor to the acryloyl carbonyl.

Identified AA local minima showed a wider range of both energies and dihedral angles. As with MA, the "global" minimum had the phosphoryl group acting as a hydrogen-bond donor to the acryloyl carbonyl oxygen. However, optimized dihedral angles fell into two groups: ±2° (the lowest-energy structures) and ±130°. Structures in which the acryloyl group was twisted ±130° lay approximately 3.5 kcal/mol above the global minimum (Figure 7).

These calculations confirm that the lowest-energy conformations of the acryloyl and methacryloyl groups (in AA and MA, respectively) differ in the coplanarity of the vinyl and carbonyl moieties as measured by the dihedral angle C(1)═C(2)—C(3)═O(4) (φ). In AA, the vinyl and carbonyl groups are essentially coplanar ($\varphi = 0°$) while in MA they are non-coplanar ($\varphi = 120°$) (Figure 7). This nonplanarity of the acrylic moiety in MA deactivates the double bond, which is consistent with the experimentally observed lack of polymerization for methacrylated glyphosate. Figure 8 shows the optimized structures of the lowest-energy conformations for MA and AA.

Biological Activity of AA and Its Polymer. Results of the biological activity trials are summarized in Table 1. The difference in growth response of *Synechococcus* 7002 after treatment with herbicides is shown in Figure 9. Both glyphosate and acrylated glyphosate display approximately equal inhibition of growth in both strains of cyanobacteria and CD 1 Red (Table 1). These data clearly demonstrate that the newly synthesized polymerizable acrylated glyphosate derivative possesses herbicidal activity similar to that of the unfunctionalized glyphosate. The residual salt present in the glyphosate sample had no effect on the media growth as was demonstrated by NaCl control experiments for *Synechococcus* 7002 (Figure 9).

Inhibition of the growth of *E. coli* was observed only during the first 10 h of incubation. Beyond 24 h of media growth, the optical density of the treated samples matched that of the controls. Therefore, both glyphosate and its acrylated derivative do not display reasonable toxicity toward *E. coli.* However, the agar experiments show a significant difference between the number of *E. coli* colonies in treated samples (11, glyphosate; 6, AA) and those in controls (36 colonies).

Synechocystos 6803, *Synechococcus* 7002, and CD 1 Red agar plates treated with glyphosate, acrylated glyphosate, and a homopolymer of acrylated glyphosate showed complete inhibition of growth and bleaching of the culture compared to the control sample. As an example, the test results for the Petri

dish surfaces coated with a polymeric AA film cast from an aqueous solution relative to the control are shown in Figure 10. These results suggest that the homopolymer of AA also possesses herbicidal activity toward cyanobacteria and algae.

The herbicidal activity of novel compounds was further elucidated by additional Kirby−Bauer tests. The capabilities of novel compounds in inhibiting the growth of the tested cyanobacteria and algae on solid media are listed in Table 2.

On the basis of the Kirby−Bauer test results it is concluded that acrylated glyphosate displays herbicidal activity that is lower than that of the parent glyphosate but higher than that of the control acrylamide. Poly(acrylated glyphosate) also possesses fairly high herbicidal activity against cyanobacteria and algae.

In summary, new polymerizable derivatives of glyphosate were synthesized and results of biological tests confirmed herbicidal activity. This type of biologically active acrylic monomer has a valuable potential for the development of new bioactive coatings with herbicidal properties.

Acknowledgment. The authors are grateful to Maria Baranova and Professor George Bullerjahn for help in conducting the biological activity tests. We thank Professor Bullerjahn and Professor Michael McKay for providing the cultures from their collections. The authors thank the Office of Naval Research for financial support (Grant No. N00014-04-1-0406). We thank Bluffton University for granting a sabbatical to D.B. and for providing the computational resources.

Supporting Information Available. Additional NMR spectra, additional results of computational studies, results of AA homopolymer molecular mass determination, and compositions of biological growth media. This material is available free of charge via the Internet at http://pubs.acs.org.

References and Notes

(1) Franz, J. E. U. S. Patent 3,799,758, March 26, 1974.
(2) Franz, J. E. U. S. Patent 3,853,530, Dec 10, 1974.
(3) Appleton, T. G.; Byriel, K. A.; Hall, J. R.; Kennard, C. H. L.; Lynch, D. E.; Sinkinson, J. A.; Smith, G *Inorg. Chem.* **1994**, *33*, 444−455.
(4) Gough, S. T. D. U.S. Patent 4,364,767, Dec 21, 1982.
(5) Ma, J.; Xu, L.; Wang, S. *Weed Sci.* **2002**, *50*, 555−559.
(6) Bauer, A. W.; Kirby, W. M.; Sherris, J. C. *Am. J. Clin. Pathol.* **1966**, *45*, 493−496.
(7) Knuuttila, P.; Knuuttila, H. *Acta Chem. Scand., Ser. B* **1979,** *33*, 623−626.
(8) Pontikis, R.; Benhida, R.; Aubertin, A.-M.; Grierson, D.; Monneret, C. *J. Med. Chem.* **1997,** *I40*, 1845−1854.
(9) Riebel, H.-J. PCT Int. Appl. WO 97/31534, Sept 4, 1997.
(10) Hideo Miyata, K.; Toru Sasaki, F.; Kohei Morikawa, K. U. S. Patent 5,859,289, Jan 12, 1999.
(11) Eliel, E. L.; Wilen, S. H.; Mander, C. N. *Stereochemistry of Organic Compounds*; John Wiley & Sons: New York, 1994; pp 550−555.
(12) Silverstein, R.; Webster, F. *Spectrometric Identification of Organic Compounds*, 6th ed.; John Wiley & Sons: New York, 1997; pp 170−178.
(13) Spectral Database System Home Page. http://www.aist.go.jp/RIODB/SDBS/cgi-bin/cre_index.cgi.
(14) Akitt, J. W. *NMR and Chemistry: An Introduction to Modern NMR Spectroscopy*, 3rd ed.; Chapman and Hall: London, 1992, pp 135−158.
(15) Sokolova, T.; Chetyrkina, G. *Vysokomol. Soedin.* **1961,** *3*, 244−247.

BM060477O